

# The $B^+ \rightarrow J/\psi\omega K^+$ reaction and $D^*\bar{D}^*$ molecular states

L. R. Dai,<sup>1,2,\*</sup> G. Y. Wang,<sup>3</sup> X. Chen,<sup>1</sup> E. Wang,<sup>3,†</sup> E. Oset,<sup>2,‡</sup> and D. M. Li<sup>3</sup>

<sup>1</sup>*Department of Physics, Liaoning Normal University, Dalian 116029, China*

<sup>2</sup>*Departamento de Física Teórica and IFIC,*

*Centro Mixto Universidad de Valencia-CSIC,*

*Institutos de Investigación de Paterna,*

*Aptdo. 22085, 46071 Valencia, Spain*

<sup>3</sup>*School of Physics and Engineering,*

*Zhengzhou University, Zhengzhou, Henan 450001, China*

(Dated: September 11, 2018)

## Abstract

We study the  $B^+ \rightarrow J/\psi\omega K^+$  reaction, and show that it is driven by the presence of two resonances, the  $X(3940)$  and  $X(3930)$ , that are of molecular nature and couple most strongly to  $D^*\bar{D}^*$ , but also to  $J/\psi\omega$ . Because of that, in the  $J/\psi\omega$  mass distribution we find a peak related to the excitation of the resonances and a cusp with large strength at the  $D^*\bar{D}^*$  threshold.

---

\* [dair@lnnu.edu.cn](mailto:dair@lnnu.edu.cn)

† [wangen@zzu.edu.cn](mailto:wangen@zzu.edu.cn)

‡ [oset@ific.uv.es](mailto:oset@ific.uv.es)

## I. INTRODUCTION

In the last decades, many hadron resonances have been observed experimentally, and some of them can not be explained as conventional mesons and baryons[1]. There exist different theoretical interpretations on the nature of these states, such as molecular, hybrid, multi-quark state, threshold enhancements, and so on [2]. As one of the popular interpretations, molecular states have long been an important subject in hadron physics [3].

However, it is not always easy to firmly identify some states as of molecular nature because of the existence of other interpretations, such as standard  $q\bar{q}(qqq)$  or multi-quark states [2, 4]. One of the defining features associated to the molecular states that couple to several hadron-hadron channels is that one can find a strong and unexpected cusp in one of the weakly coupled channels at the threshold of the channels corresponding to the main component of the molecular state [5, 6].

A recent example of this feature is found in the  $B^+ \rightarrow J/\psi\phi K^+$  decay measured by the LHCb collaboration [7, 8]. The LHCb analysis, including only the  $X(4140)$  resonance at low  $J/\psi\phi$  invariant masses, results in a width for the  $X(4140)$  resonance much larger than the average of the PDG [1]. We have studied this reaction, taking into account the molecular state  $X(4160)$ , in addition to the  $X(4140)$  resonance, and provided a better description of the low  $J/\psi\phi$  mass distribution [6]. According to Ref. [9], the  $X(4160)$  state is a  $D_s^*\bar{D}_s^*$  state with  $I^G(J^{PC}) = 0^+(2^{++})$  and couples to  $J/\psi\phi$ . As a result, the  $J/\psi\phi$  mass spectrum develops a strong cusp at the  $D_s^*\bar{D}_s^*$  threshold. A similar structure is also seen, although with poor statistics, in the recent BESIII work on the  $e^+e^- \rightarrow \gamma J/\psi\phi$  [10], and the corresponding discussion can be seen in Ref. [11].

In Ref. [9], two  $D^*\bar{D}^*$  molecular states were found as  $I^G(J^{PC}) = 0^+(0^{++})$  and  $0^+(2^{++})$  at 3943 and 3922 MeV, respectively. In addition to the strongly coupled channel  $D^*\bar{D}^*$ , both states also couple to  $J/\psi\omega$  in the second place. In order to show the features of the molecular nature of these two resonances, we studied the  $B_c^- \rightarrow \pi^- J/\psi\omega$  reaction, and found a peak around 3920  $\sim$  3940 MeV, corresponding to the excitation of these two resonances, and a cusp with large strength at the  $D^*\bar{D}^*$  threshold, in the  $J/\psi\omega$  invariant mass distribution [5].

In Ref. [12] one finds the  $J/\psi\omega$  invariant mass distribution for the  $B^+ \rightarrow J/\psi\omega K^+$  reaction using data collected by the LHCb experiment <sup>1</sup>, which is used to search for exotic

---

<sup>1</sup> We are thankful to G. Andreassi for allowing us to use the data of his PhD dissertation [12].

states, in particular the  $X(3872)$ . If we look at Fig. 4.1 of Ref. [12], a peak presumably due to the excitation of  $X(3872)$  is observed, but another peak around 3920 ~ 3940 MeV and a cusp-like structure around the 4020 MeV, the threshold of  $D^*\bar{D}^*$ , are also seen, which are similar to the features we found in the  $J/\psi\omega$  invariant mass distribution of the  $B_c^- \rightarrow \pi^- J/\psi\omega$  reaction [5]. It should be noted that, in Ref. [12], the peak around 3920 ~ 3940 MeV is associated to the  $\chi_{c0}(2P)$ , with the fitted mass 3915 MeV. However, there is a debate about the mass of the  $\chi_{c0}(2P)$  [2, 13], and the decay channel  $J/\psi\omega$  of  $\chi_{c0}(2P)$  is OZI suppressed. In addition, prior to Ref. [12], Belle and Babar collaborations also found peaks in the 3920 ~ 3940 MeV region of the  $J/\psi\omega$  mass distribution for this reaction [14, 15], and the resonance associated to the peak has a mass of  $3943 \pm 11 \pm 13$  MeV in the analysis of Belle collaboration [14].<sup>2</sup> Thus, it is straightforward to analyze the  $B^+ \rightarrow J/\psi\omega K^+$  reaction by considering the two  $D^*\bar{D}^*$  molecular states found in Ref. [9].

In this work, we will investigate the  $J/\psi\omega$  interaction in the  $B^+ \rightarrow J/\psi\omega K^+$  reaction, and show that the peak around 3920 ~ 3940 MeV, together with the cusp around  $D^*\bar{D}^*$  threshold, can be tied to the  $D^*\bar{D}^*$  molecular structure of the two states.

This paper is organized as follows. In Sec. II, we present the mechanisms of the  $B^+ \rightarrow J/\psi\omega K^+$  reaction, our results and discussions are given in Sec. III. Finally, a short summary is given in Sec. IV.

## II. FORMALISM

In order to deal with a quark  $b$  rather than  $\bar{b}$ , we study the complex conjugate reaction of  $B^+ \rightarrow J/\psi\omega K^+$ ,  $B^- \rightarrow J/\psi\omega K^-$ . To see how the  $B^- \rightarrow J/\psi\omega K^-$  reaction proceeds, we look at the possible Cabibbo-favored mechanisms at the quark level. They are depicted in Figs.1(a), 1(b) and 1(c). The mechanisms of Figs.1(a) and 1(b) imply internal emission followed by hadronization of a primary  $q\bar{q}$  component by an extra  $\bar{q}q$  component with the quantum numbers of the vacuum. In Fig.1(a) the primary  $s\bar{u}$  component is hadronized with  $u\bar{u}$  and we then get  $\omega K^-$  together with  $c\bar{c}$  that leads to  $J/\psi$ . In Fig.1(b) we hadronize the  $c\bar{c}$  component and we can get  $D^*\bar{D}^*$  together with  $s\bar{u}$  that leads to  $K^-$ . This is not the  $J/\psi\omega K^-$  state that one observes, but the idea is that the  $D^*\bar{D}^*$  will interact and create a

<sup>2</sup> Because of the large bin size of the Belle and Babar data ( $\sim 50$  MeV), both the  $J/\psi\omega$  mass distributions do not show a significant cusp around the  $D^*\bar{D}^*$  threshold, and we do not consider the data of Belle and Babar collaboration in this work.

resonance that couples to  $J/\psi\omega$ .

In Fig.1(c) we have the mechanism of external emission, which is color-favored with respect to internal emission. Here the primary  $s\bar{c}$  pair is hadronized and we get also a  $\bar{D}^{*0}K^-$  component together with  $D^{*0}$  from the remaining  $c\bar{u}$  pair. Once again the  $\bar{D}^{*0}D^{*0}$  pair interacts to produce  $J/\psi\omega$  at the end.

It is instructive to see which are the most important mechanisms of those discussed above. One is tempted to choose the one in Fig.1(a) that produces the  $J/\psi\omega K^-$  without the need of rescattering. However, since the interaction of  $D^*\bar{D}^*$  produces resonances, the rescattering mechanism becomes more important than the tree level direct production in the energy region of the  $D^*\bar{D}^*$  resonant states. To see this, let us see the meson decomposition of Fig.1(b). Hadronizing with  $\bar{u}u$  the  $c\bar{c}$  component we get  $D^{*0}\bar{D}^{*0}$ , hadronizing with  $\bar{d}d$  we obtain  $D^{*+}D^{*-}$  and hadronizing with  $\bar{s}s$  we obtain  $D_s^{*+}D_s^{*-}$ , and, hence, we get the combination  $D^{*0}\bar{D}^{*0} + D^{*+}D^{*-} + D_s^{*+}D_s^{*-}$ . With the phase convention for isospin ( $D^{*+}, -D^{*0}$ ), ( $\bar{D}^{*+}, D^{*-}$ ) we have the isospin  $I = 0$  combination.

$$D^{*0}\bar{D}^{*0}(I = 0) = \frac{1}{\sqrt{2}}(D^{*+}D^{*-} + D^{*0}\bar{D}^{*0}). \quad (1)$$

Then we look at the rescattering diagrams of Fig.2 creating the  $I^G[J^{PC}] = 0^+[0^{++}]$  resonance  $X(3940)$  and decaying to  $J/\psi\omega$ . With the  $J/\psi\omega$  and  $D^*\bar{D}^*$  loop functions of the same size, the ratio of amplitudes of Fig. 2 (a) versus Fig.2 (b) is

$$\left| \frac{t(2a)}{t(2b)} \right| \simeq \left| \frac{g_{R,J/\psi\omega}}{\sqrt{2}g_{R,D^*\bar{D}^*}(I = 0)} \right|. \quad (2)$$

In Table I we give the couplings of this resonance to the different coupled channels extracted from [16]. We find then that

$$\left| \frac{t(2a)}{t(2b)} \right| \simeq 5\%. \quad (3)$$

We see that this magnitude is small and as a consequence, we neglect the mechanism of Fig.1(a) and Fig.2 (a) from our study. A similar conclusion can be reached about the tensor  $0^+[2^{++}]$  resonance  $X(3930)$ . We show the couplings of this latter resonance to the different coupled channels of [16] in Table II. We have neglected the  $D_s^{*+}D_s^{*-}$  channel for the counting of Eq.(3), which, if considered, renders the ratio of Eq.(3) even smaller. The diagram of Fig.1(c) corresponds to the color-favored external emission mechanism, which is usually enhanced by a factor of three with respect to the internal emission [17] and also

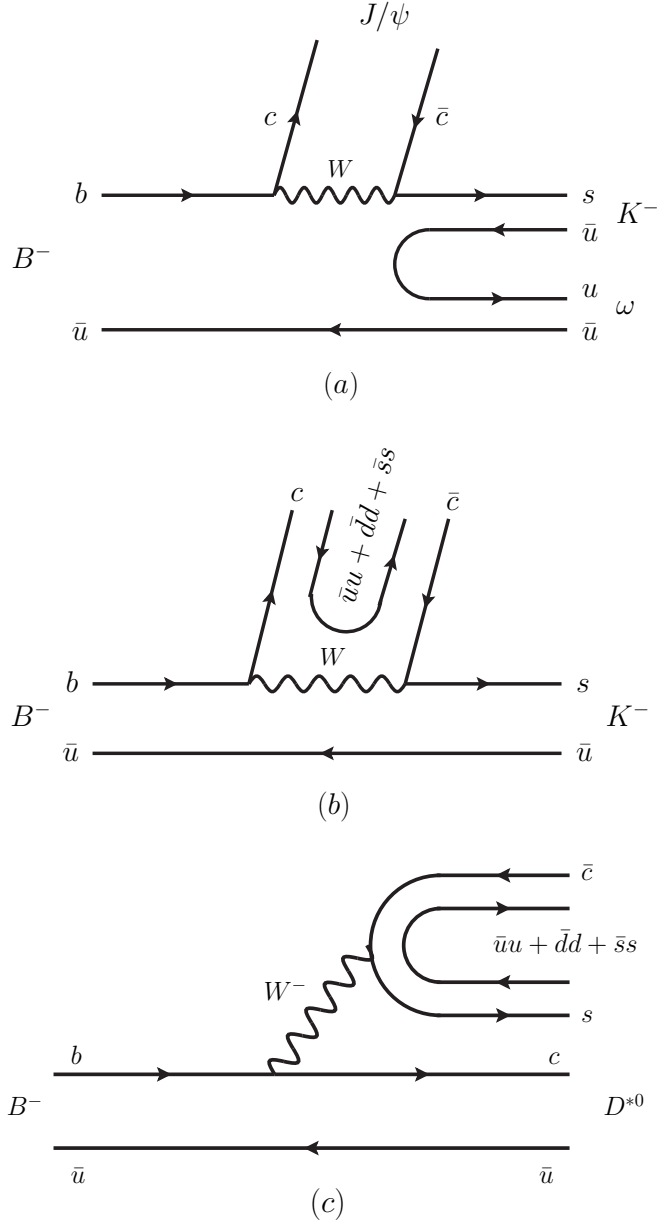


FIG. 1. The internal emission mechanism at the microscopic quark picture. (a) The  $B^- \rightarrow J/\psi s\bar{u}$  decay and hadronization of  $s\bar{u}$  through  $\bar{q}q$  creation with vacuum quantum numbers; (b)  $B^- \rightarrow K^- c\bar{c}$  decay and hadronization of  $c\bar{c}$  through  $\bar{q}q$ ; (c) The external emission mechanism and hadronization of the  $s\bar{c}$  pair with  $q\bar{q}$ .

usually interferes constructively [18]. We will assume that this is the case here too, but will play with uncertainties on the relative weight of both mechanisms. With the hadronization coming from Figs. 1(b) and 1(c) that we consider, we have the hadronic state  $|H\rangle$  produced

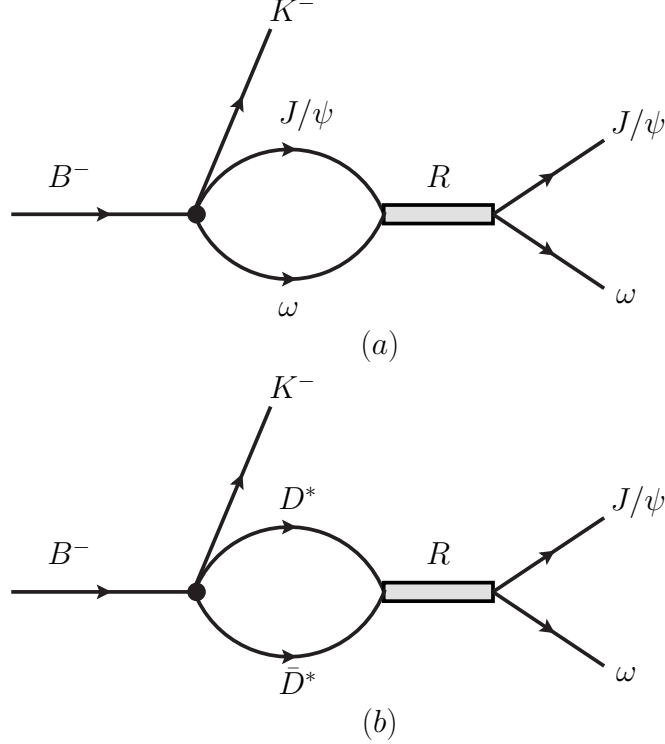


FIG. 2. Interaction mechanism to produce the  $J/\psi\omega$  final state (a) through rescattering of  $J/\psi\omega$  components; (b) through rescattering of  $D^*\bar{D}^*$  components.  $R$  is either the  $X(3922) (2^{++})$  or  $X(3943) (0^{++})$ .

before rescattering

$$\begin{aligned}
 |H\rangle &= |(D^{*0}\bar{D}^{*0} + D^{*+}\bar{D}^{*-} + D_s^{*+}\bar{D}_s^{*-} + 3C D^{*0}\bar{D}^{*0})K^- \rangle \\
 &= |[(1 + 3C)D^{*0}\bar{D}^{*0} + D^{*+}\bar{D}^{*-} + D_s^{*+}\bar{D}_s^{*-}] K^- \rangle.
 \end{aligned}
 \tag{4}$$

With these primary components we shall take into account rescattering, which is depicted in Fig. 3, where  $R$  will stand for any of the two resonances that we produce with these channels. We will vary the value of  $C$  around unity, but we can anticipate that it hardly changes the shape of the distribution obtained. The minor changes of the shape by changing  $C$  are due to the presence of the  $D_s^{*+}\bar{D}_s^{*-}$  channel, which is not very important in the present case. If we remove this channel the results do not depend on  $C$ , except for a global normalization.

The combination of  $|H\rangle$  in Eq. (4) accounts only for the flavor composition. We need to take into account the spin-angular momentum structure of the vertices. For production of two vectors in  $J = 0$  we proceed in  $L = 0$  (for the kaon) to conserve angular momentum, and we have the amplitude for the  $B^- \rightarrow K^- D^{*+} \bar{D}^{*-}$

TABLE I. Couplings  $g_i$  of the  $0^{++}$  resonance to the relevant channels, in units of MeV.

$$\sqrt{s}_{pole} = 3943 + i7.4, I^G[J^{PC}] = 0^+[0^{++}]$$

channels	$g_i$	channels	$g_i$
$D^*\bar{D}^*$	$18810 - i682$	$\phi\phi$	$-1000 - i150$
$D_s^*\bar{D}_s^*$	$8426 + i1933$	$J/\psi J/\psi$	$417 + i64$
$K^*\bar{K}^*$	$10 - i11$	$\omega J/\psi$	$-1429 - i216$
$\rho\rho$	$-22 + i47$	$\phi J/\psi$	$889 + i196$
$\omega\omega$	$1348 + i234$	$\omega\phi$	$-215 - i107$

TABLE II. Couplings  $g_i$  of the  $2^{++}$  resonance to the relevant channels, in units of MeV.

$$\sqrt{s}_{pole} = 3922 + i26, I^G[J^{PC}] = 0^+[2^{++}]$$

channels	$g_i$	channels	$g_i$
$D^*\bar{D}^*$	$21100 - i1802$	$\phi\phi$	$-904 - i1783$
$D_s^*\bar{D}_s^*$	$1633 + i6797$	$J/\psi J/\psi$	$1783 + i197$
$K^*\bar{K}^*$	$42 + i14$	$\omega J/\psi$	$-2558 - i2289$
$\rho\rho$	$-75 + i37$	$\phi J/\psi$	$918 + i2921$
$\omega\omega$	$1558 + i1821$	$\omega\phi$	$91 - i784$

$$A' \vec{\epsilon} \cdot \vec{\epsilon}', \quad (5)$$

with  $\vec{\epsilon}, \vec{\epsilon}'$  the polarization vectors of  $D^*, \bar{D}^*$ . Note that we shall work in the rest frame of the resonances produced, where  $D^*, \bar{D}^*$  momenta are small with respect to their masses and then we neglect the  $\epsilon^0$  component. This is actually very accurate for these momenta as can be seen in Appendix A of [19].

On the other hand, in the channel of  $VV$  with  $J = 2$  we need  $L = 2$  to match the angular momentum of the  $B^-$ , and this leads to the amplitude

$$B (\vec{\epsilon} \cdot \vec{k} \vec{\epsilon}' \cdot \vec{k} - \frac{1}{3} |\vec{k}|^2 \vec{\epsilon} \cdot \vec{\epsilon}'), \quad (6)$$

where  $\vec{k}$  is the momentum of the kaon in the  $J/\psi\omega$  rest frame. Hence, the tree level ampli-

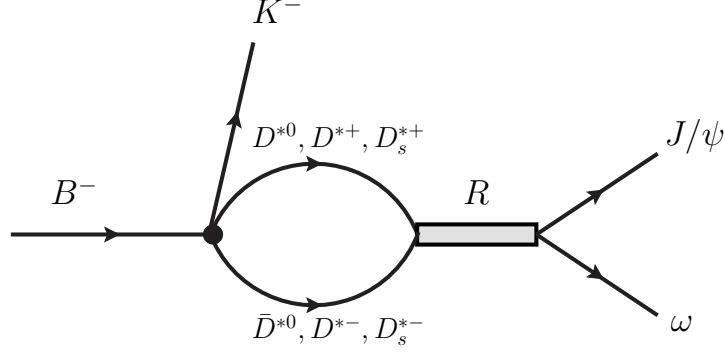


FIG. 3. Mechanism to produce the  $J/\psi\omega$  final state through rescattering of  $D^0\bar{D}^0$ ,  $D^{*+}\bar{D}^{*-}$ , and  $D_s^{*+}\bar{D}_s^{*-}$  components.

tudes are given by

$$\begin{aligned}
t_{B^- \rightarrow K^- D^{*0} \bar{D}^{*0}}^{tree} &= \left[ A |\vec{k}_{av}|^2 \vec{\epsilon} \cdot \vec{\epsilon}' \right. \\
&\quad \left. + B (\vec{\epsilon} \cdot \vec{k} \vec{\epsilon}' \cdot \vec{k} - \frac{1}{3} |\vec{k}|^2 \vec{\epsilon} \cdot \vec{\epsilon}') \right] (1 + 3C), \\
t_{B^- \rightarrow K^- D^{*+} D^{*-}}^{tree} &= A |\vec{k}_{av}|^2 \vec{\epsilon} \cdot \vec{\epsilon}' \\
&\quad + B (\vec{\epsilon} \cdot \vec{k} \vec{\epsilon}' \cdot \vec{k} - \frac{1}{3} |\vec{k}|^2 \vec{\epsilon} \cdot \vec{\epsilon}'), \\
t_{B^- \rightarrow K^- D_s^{*+} D_s^{*-}}^{tree} &= A |\vec{k}_{av}|^2 \vec{\epsilon} \cdot \vec{\epsilon}' \\
&\quad + B (\vec{\epsilon} \cdot \vec{k} \vec{\epsilon}' \cdot \vec{k} - \frac{1}{3} |\vec{k}|^2 \vec{\epsilon} \cdot \vec{\epsilon}'), \tag{7}
\end{aligned}$$

where we have substituted  $A'$  of Eq.(5) by  $A|\vec{k}_{av}|^2$  with  $\vec{k}_{av}$ , an average value of  $\vec{k}$ , just to make  $A$  and  $B$  with the same dimension. We take  $|\vec{k}_{av}| = 1000$  MeV.

Next, we take into account the rescattering depicted in Fig. 3 to get  $K^- J/\psi\omega$  in the final state and we find the amplitude for  $J/\psi\omega$  production

$$t_{J/\psi\omega} = A |\vec{k}_{av}|^2 \vec{\epsilon} \cdot \vec{\epsilon}' t_1 + B (\vec{\epsilon} \cdot \vec{k} \vec{\epsilon}' \cdot \vec{k} - \frac{1}{3} |\vec{k}|^2 \vec{\epsilon} \cdot \vec{\epsilon}') t_2, \tag{8}$$

where  $t_1$  and  $t_2$  are given by

$$\begin{aligned}
t_1 &= G_{D^{*0}\bar{D}^{*0}}(M_{inv}) t_{D^{*0}\bar{D}^{*0} \rightarrow J/\psi\omega}^I (1 + 3C) \\
&\quad + G_{D^{*+}D^{*-}}(M_{inv}) t_{D^{*+}D^{*-} \rightarrow J/\psi\omega}^I \\
&\quad + G_{D_s^{*+}D_s^{*-}}(M_{inv}) t_{D_s^{*+}D_s^{*-} \rightarrow J/\psi\omega}^I, \tag{9}
\end{aligned}$$



$$\begin{aligned}
t_2 &= G_{D^*0\bar{D}^*0}(M_{\text{inv}}) t_{D^*0\bar{D}^*0\rightarrow J/\psi\omega}^{II} (1 + 3C) \\
&+ G_{D^{*+}D^{*-}}(M_{\text{inv}}) t_{D^{*+}D^{*-}\rightarrow J/\psi\omega}^{II} \\
&+ G_{D_s^{*+}D_s^{*-}}(M_{\text{inv}}) t_{D_s^{*+}D_s^{*-}\rightarrow J/\psi\omega}^{II}, \tag{10}
\end{aligned}$$

with  $t^I$  the amplitude for the scalar resonance  $J^{PC} = 0^{++}$ , 3940 MeV and  $t^{II}$  for the tensor resonance  $J^{PC} = 2^{++}$ , 3930 MeV.

Since the  $\vec{\epsilon} \cdot \vec{\epsilon}'$  and  $\vec{\epsilon} \cdot \vec{k} \vec{\epsilon}' \cdot \vec{k} - \frac{1}{3}|\vec{k}|^2 \vec{\epsilon} \cdot \vec{\epsilon}'$  structures filter spin 0 and 2 respectively, the structure is kept in the iterations implicit in Eqs. (9) and (10). The  $G$  functions in the former equations are the vector-vector loop functions for the intermediate  $D^*\bar{D}^*$ ,  $D_s^*\bar{D}_s^*$  in Fig. 3. They are regularized in [16] using dimensional regularization with the subtraction constant  $a = -2.07$  and  $\mu = 1000$  MeV. Here, we follow the prescription of [5, 6] and we use the cutoff method with  $q_{max}$  fixed to reproduce the results of [16]. In the former equations  $A$  and  $B$  are functions (we take them as constants in the limited range of invariant mass studied) which have to do with the weight of the weak process and hadronization before the final state interaction is taken into account. We shall vary  $A$  and  $B$  within a reasonable range to see the results.

With the amplitudes of Eq. (8) the mass distributions, summing  $|t|^2$  over the final vector polarizations, is given by

$$\begin{aligned}
\frac{d\Gamma}{dM_{\text{inv}}^{J/\psi\omega}} &= \frac{1}{(2\pi)^3} \frac{1}{4M_B^2} k' \tilde{p}_\omega \\
&\times \left( 3|A|^2 |\vec{k}_{\text{av}}|^4 |t_1|^2 + \frac{2}{3}|B|^2 |\vec{k}|^4 |t_2|^2 \right), \tag{11}
\end{aligned}$$

where  $k'$  is the kaon momentum in the  $B^-$  rest frame,  $\tilde{p}_\omega$  the  $\omega$  momentum in the  $J/\psi\omega$  rest frame and  $k$  the kaon momentum in the  $J/\psi\omega$  rest frame for the  $J/\psi\omega$  final state,

$$\begin{aligned}
k' &= \frac{\lambda^{1/2}(M_{B^-}^2, m_K^2, M_{\text{inv}}^2)}{2M_{B^-}}, \\
k &= \frac{\lambda^{1/2}(M_{B^-}^2, m_K^2, M_{\text{inv}}^2)}{2M_{\text{inv}}}, \\
\tilde{p}_\omega &= \frac{\lambda^{1/2}(M_{\text{inv}}^2, m_{J/\psi}^2, m_\omega^2)}{2M_{\text{inv}}}. \tag{12}
\end{aligned}$$

Next we need the amplitudes  $t^I$  and  $t^{II}$  obtained from [16], in which the Flatté form of the amplitude was used in terms of the couplings and the width. We have listed the couplings in Table I and II.

The amplitudes are,  $i = I$  or  $II$ , given by

$$\begin{aligned}
t_{D^{*0}\bar{D}^{*0}, J/\psi\omega}^i &= \frac{\frac{1}{\sqrt{2}}g_{R, D^*\bar{D}^*}^{(i)} g_{R, J/\psi\omega}^{(i)}}{M_{\text{inv}}^2 - M_{R_i}^2 + iM_{R_i}\Gamma_{R_i}}, \\
t_{D^{*+}D^{*-}, J/\psi\omega}^i &= \frac{\frac{1}{\sqrt{2}}g_{R, D^*\bar{D}^*}^{(i)} g_{R, J/\psi\omega}^{(i)}}{M_{\text{inv}}^2 - M_{R_i}^2 + iM_{R_i}\Gamma_{R_i}}, \\
t_{D_s^{*+}D_s^{*-}, J/\psi\omega}^i &= \frac{g_{R, D_s^{*+}D_s^{*-}}^{(i)} g_{R, J/\psi\omega}^{(i)}}{M_{\text{inv}}^2 - M_{R_i}^2 + iM_{R_i}\Gamma_{R_i}},
\end{aligned} \tag{13}$$

where the width  $\Gamma_{R_i}$  is taken as

$$\Gamma_{R_i} = \Gamma_0^{(i)} + \Gamma_{J/\psi\omega}^{(i)} + \Gamma_{D^*\bar{D}^*}^{(i)}, \tag{14}$$

with

$$\Gamma_{J/\psi\omega}^{(i)} = \frac{|g_{R, J/\psi\omega}^i|^2}{8\pi M_{R_i}^2} \tilde{p}_\omega, \tag{15}$$

and  $\tilde{p}_\omega$  given by Eq. (12) as a function of  $M_{\text{inv}}$ , and

$$\Gamma_{D^*\bar{D}^*}^{(i)} = \frac{|g_{R, D^*\bar{D}^*}^i|^2}{8\pi M_{R_i}^2} \tilde{p}_{D^*} \Theta(M_{\text{inv}} - 2M_{D^*}), \tag{16}$$

with  $\tilde{p}_{D^*}$  as  $\tilde{p}_\omega$  in Eq. (12) with the changes  $M_{J/\psi} \rightarrow M_{D^*}$ ,  $M_\omega \rightarrow M_{\bar{D}^*}$ . The width  $\Gamma_0^{(i)}$  in Eq. (14) accounts for the channels different of  $J/\psi\omega$  and  $D^*\bar{D}^*$ , mostly the light channels, such that  $\Gamma_0^{(i)}$  is practically constant and we take

$$\Gamma_0^{(i)} = \Gamma_{R_i} - \Gamma_{J/\psi\omega}^{(i)}(M_{\text{inv}}^{J/\psi\omega} = M_{R_i}). \tag{17}$$

Note that in Eq. (16),  $\Gamma_{D^*\bar{D}^*}^{(i)}$  only starts above the  $D^*\bar{D}^*$  threshold, but since the coupling of the resonance to this channel is so large, it grows fast above threshold giving rise to the Flatté effect.

### III. RESULTS

We will present the invariant mass distribution  $\frac{d\Gamma}{dM_{\text{inv}}^{J/\psi\omega}}$  in arbitrary units. Since  $A$  and  $B$  have been normalized to have the same dimensions, the two terms in Eq. (11) have similar strength for  $A = B$ . For this purpose, we take  $A = 1$  and look at the results for different values of  $B$ . As discussed in [5],  $\frac{B}{A}$  should be bigger than 1, so we take the ratio of 1.5, 2, 5. As mentioned above, we also look at the results for different values of  $C$ .

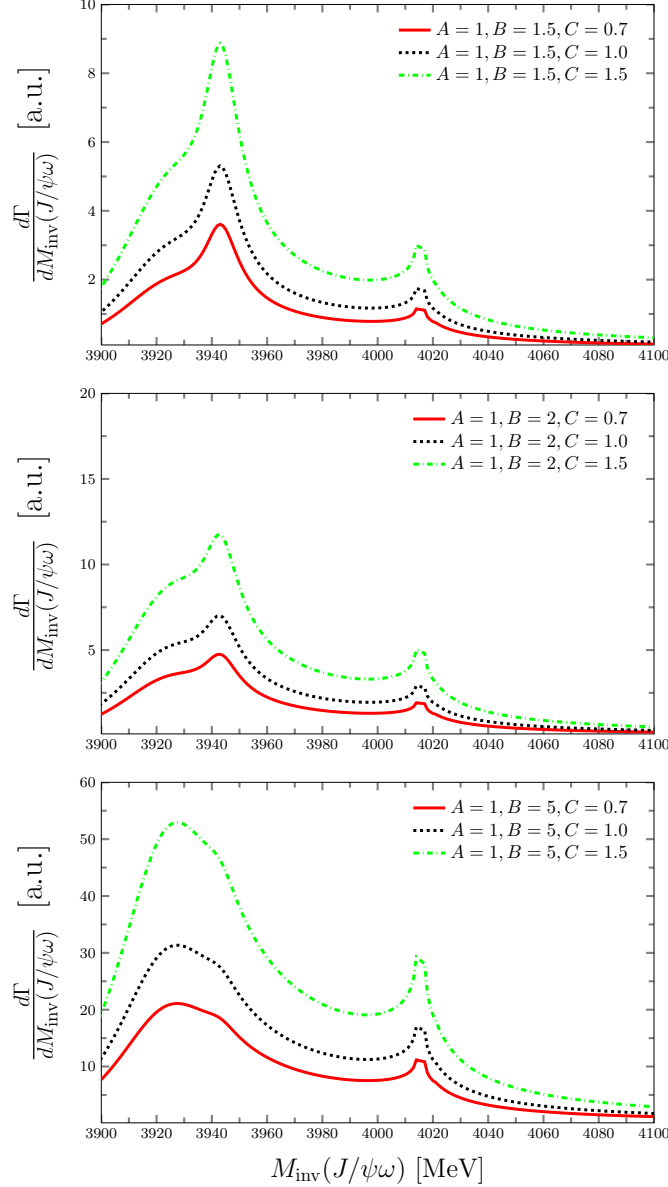


FIG. 4.  $\frac{d\Gamma}{dM_{inv}^{J/\psi\omega}}$  the results for the different values of the parameter  $B$  and  $C$ .

We show in Fig.4 the results of  $\frac{d\Gamma}{dM_{inv}^{J/\psi\omega}}$  for these different values. The absolute normalization is arbitrary and the shape changes a bit since one gives more strength to one or another resonance changing  $B$  and  $C$ . From Fig.4 we can see that due to the proximity of the two resonances, and the fact that both of them can be produced in this reaction, the two peaks actually merge into a broader one, although a precise measurement could maybe allow a separation of the two peaks, particularly if a partial wave analysis is done that separates the two different spin resonances. Interesting, however, is the fact that the cusp appears always

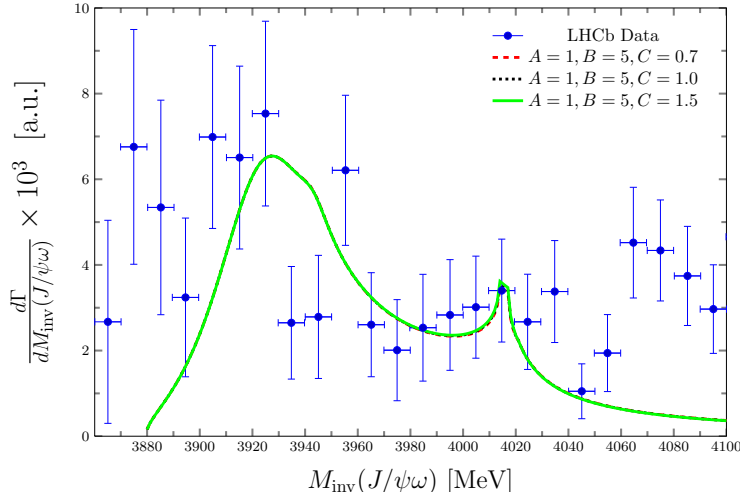


FIG. 5. Fitted  $J/\psi\omega$  invariant mass distribution to LHCb data [12] for  $B^+ \rightarrow J/\psi\omega K^+$  reaction with different parameters  $B$  and  $C$ ,  $A$  is normalized.

at the same place, the  $D^*\bar{D}^*$  threshold. The other relevant feature is that its strength grows with increasing weight of the tensor resonance, indicating that the cusp is basically tied to the  $2^{++}$   $X(3930)$  state.

In Fig. 5 we compare our results with the data of Ref. [12]. We have chosen  $B = 5$ , which gives a better reproduction of the data. The peak is due mostly to the tensor  $X(3930)$  state and qualitatively accounts for the strength around 3900 MeV observed in the experiment. The other feature coming from our framework is the unavoidable cusp at the  $D^*\bar{D}^*$  threshold. The data have large errors but a fall down of the distribution beyond this threshold is present in the data before it starts growing again, probably due to the excitation of other resonances that are of a different nature than the two discussed here. One should note the similarity of this feature with the cusp at the  $D_s^*\bar{D}_s^*$  threshold observed in the  $B^+ \rightarrow J/\psi\omega K^+$  experiment [8], which was interpreted in [6] in terms of resonances that couple to  $D_s^*\bar{D}_s^*$ . The data also seems to indicate the contribution of another resonance around 3875 MeV, which is most probably the  $X(3872)$ . Once again, better statistics and partial wave analyses will help shedding further light on this issue.

It could be most useful to get better data for this distribution, and the present work should serve as a motivation for it. Given the interpretation of the  $B^+ \rightarrow J/\psi\omega K^+$  data presented here, and its relevance to learn about the nature of some resonances, it would be

most advisable to increase the statistics in this reaction to improve the present precision.

#### IV. CONCLUSIONS

We have presented a theoretical interpretation of the data on the  $B^+ \rightarrow J/\psi\omega K^+$  reaction [12] in the range of  $J/\psi\omega$  invariant mass 3900  $\sim$  4050 MeV. In this range we find two resonances  $X(3930)$  and  $X(3940)$  that couple strongly to  $D^*\bar{D}^*$  in  $J^{PC} = 2^{++}, 0^{++}$  respectively. The excitation of these resonances particularly the  $X(3930)$  gives rise to a peak that accounts for the large experimental strength around 3900 MeV. The other feature is the unavoidable presence of a strong cusp at the  $D^*\bar{D}^*$  threshold, which seems to be supported by experiment. This behaviour is reminiscent of the one observed in the  $B^+ \rightarrow J/\psi\omega K^+$  reaction where a cusp is observed at the  $D_s^*\bar{D}_s^*$  threshold, and which, similarly to the present case, could also be interpreted in terms of resonances coupled strongly to  $D_s^*\bar{D}_s^*$ . The present discussion should serve to stimulate further experimental work, improving the statistics and disentangling the quantum numbers of the structure observed.

#### ACKNOWLEDGEMENTS

LRD wishes to acknowledge the support from the National Natural Science Foundation of China (No. 11575076) and the State Scholarship Fund of China (No. 201708210057). This work is partly supported by National Natural Science Foundation of China (No. 11505158). This work is partly supported by the Spanish Ministerio de Economía y Competitividad and European FEDER funds under Contracts No. FIS2017-84038-C2-1-P B and No. FIS2017-84038-C2-2-P B, and the Generalitat Valenciana in the program Prometeo II-2014/068, and the project Severo Ochoa of IFIC, SEV-2014-0398 (EO).

- 
- [1] M. Tanabashi *et al.*, Review of Particle Physics, Phys. Rev. D **98**, no. 3, 030001 (2018).
  - [2] H. X. Chen, W. Chen, X. Liu and S. L. Zhu, Phys. Rept. **639**, 1 (2016).
  - [3] F. K. Guo, C. Hanhart, U. G. Meißner, Q. Wang, Q. Zhao and B. S. Zou, Rev. Mod. Phys. **90**, 015004 (2018).
  - [4] M. Karliner, J. L. Rosner and T. Skwarnicki, Ann. Rev. Nucl. Part. Sci. **68**, 17 (2018).

- [5] L. R. Dai, J. M. Dias and E. Oset, Eur. Phys. J. C **78**, no. 3, 210 (2018).
- [6] E. Wang, J. J. Xie, L. S. Geng and E. Oset, Phys. Rev. D **97**, 014017 (2018).
- [7] R. Aaij *et al.* [LHCb Collaboration], Phys. Rev. D **95**, 012002 (2017).
- [8] R. Aaij *et al.* [LHCb Collaboration], Phys. Rev. Lett. **118**, 022003 (2017); Phys. Rev. D **95**, 012002 (2017).
- [9] R. Molina and E. Oset, Phys. Rev. D **80**, 114013 (2009).
- [10] M. Ablikim *et al.* [BESIII Collaboration], Phys. Rev. D **97**, 032008 (2018).
- [11] E. Wang, J. J. Xie, L. S. Geng and E. Oset, arXiv:1806.05113 [hep-ph].
- [12] G. Andreassi, Search for exotic resonances in the decay  $B^+ \rightarrow J/\psi \omega K^+$  in the LHCb experiment at CERN, CERN-THESIS-2014-243.
- [13] E. J. Eichten, K. Lane and C. Quigg, Phys. Rev. D **69**, 094019 (2004).
- [14] K. Abe *et al.* [Belle Collaboration], Phys. Rev. Lett. **94**, 182002 (2005).
- [15] B. Aubert *et al.* [BaBar Collaboration], Phys. Rev. Lett. **101**, 082001 (2008).
- [16] R. Molina and E. Oset, Phys. Rev. D **80**, 114013 (2009).
- [17] L. L. Chau, Phys. Rept. **95**, 1 (1983).
- [18] W. H. Liang and E. Oset, Eur. Phys. J. C **78**, 528 (2018).
- [19] S. Sakai, E. Oset and A. Ramos, Eur. Phys. J. A **54**, 10 (2018).